

CALIBRATION OF MULTIPLE CAMERAS TO A 3D LASER RANGE FINDER

Marcel Häselich, René Bing, Dietrich Paulus

Active Vision Group, AGAS Robotics
University of Koblenz-Landau
Universitätsstr. 1, 56070 Koblenz, Germany
{mhaeselich,rbing,paulus}@uni-koblenz.de

ABSTRACT

Robots, especially autonomous systems, need a precise perception of the environment for path planning and manipulation tasks. Different sensors provide various data for this task. Camera to 3D laser range finder calibration allows algorithms to work efficiently on depth measurements, color and texture features and benefit from the signals of both sensor types at once in real-time. In this paper we describe our extensions to an existing calibration approach from Unnikrishnan and Herbert. The calibration is analyzed from a robotic perspective with focus on improving required time, practicality and simplification of the calibration. Field of application ranges from robotics and agricultural engines to industrial applications. The feasibility of the approach is discussed and resulting data fusion is presented.

Index Terms— calibration, robotics, sensor data fusion

1. INTRODUCTION

Unstructured environments pose a challenging scenario for autonomous robots. Modern 3D Laser Range Finders (LRFs) grant a detailed picture of the environment in form of distance measurements. Nevertheless, algorithms cannot determine from the distance values alone, whether a point cloud is solid and an obstacle or soft an passable area like high grass. Therefore cameras provide a perfect extension as they add color and texture to the distance measurements and thereby allow a differentiation of surfaces and objects.

Our goal is to realize a fast, feasible and portable calibration solution for our autonomous outdoor robot. For this task we extend the approach of Unnikrishnan and Herbert [1] and integrate it into our robotic framework. We accelerated the approach by an detection of the checkerboard in both the camera and laser data and created a new calibration pattern especially for this task. The resulting calibration allows an estimation of all intrinsic camera parameters and the positions and rotations of our cameras in relation to our 3D LRF.

The paper is structured as follows. Sec. 2 starts with a discussion of related work followed by a description of our sensors in Sec. 3. In Sec. 4 the calibration process is detailed and results are shown. Finally, we present the conclusion in Sec. 5.

2. RELATED WORK

Calibration of cameras with LRFs is an active research topic in robotics. A wide range of methods have been published in the last years. These approaches can be discerned by the type of the camera, e.g. pinhole or omnidirectional cameras, and the type of the LRF, e.g. 2D or 3D LRFs.

A comparison of four different calibration techniques for 3D range data and camera images is given by Cobzaş et al. [2]. The techniques cover point and line based retrieval of the rigid transformations and image based mapping between the datasets.

Zhang and Pless [3] present a method to calibrate a 2D LRF with a camera manually from multiple views. Their approach registers the laser points on a planar checkerboard pattern with the camera image of the same.

Unnikrishnan and Herbert [1] extend the approach of Zhang and Pless for the calibration of a 3D LRF with a camera. They extract a plane from four manually selected vertices on the checkerboard pattern and register it with the automatically detected pattern of the image.

Similar to the method of Unnikrishnan and Herbert works the approach presented by Andreasson et al. [4]. Andreasson et al. designed a new calibration pattern that consists of a common checkerboard framed by grey duct tape which makes the frame detectable in the intensity values of their LRF.

Leonard et al. [5] present a method for multi-sensor calibration in their technical report of the DARPA Urban Challenge. Besides various other sensors, cameras and LRFs were calibrated, too. They use a calibration object in form of a pyramid with an attached camera that can detect fiducials on their vehicle to determine the pyramids position. The result is validated with a CAD model of the vehicle.

A method to calibrate a camera to a 2D LRF is described

This work was partially funded by Wehrtechnische Dienststelle 51 (WTD), Koblenz, Germany.

by Caglioti et al. [6]. Their calibration is based on the algorithm introduced by Colombo et al. [7] and uses coaxial circles. A calibration pattern is not required, but the laser beams need to be visible in the camera images.

Núñez et al. [8] present a camera to 3D LRF calibration based on the approach of Horaud and Dornaika [9]. The authors use a squared checkerboard rotated by 45° and move their sensor platform around it. Inference about the motion is extracted from an Inertial measurement Unit (IMU).

A stereo camera is calibrated to a 2D LRF by Li et al. [10]. Their specially build calibration pattern is a black right triangle which they use to find corresponding lines in the camera image and in the laser data.

Aliakbarpour et al. [11] propose a method to calibrate a stereo camera with a 2D LRF with the help of an IMU. The approach is based on the calibration of Svoboda et al. [12], where calibration is performed with a moving light source. Aliakbarpour et al. use a common laser pointer as light source and retrieve the orientation of the LRF from the IMU.

Mei and Rives [13] present several methods to calibrate a 2D LRF with an omnidirectional camera. In order to estimate the position of the camera in relation to the LRF, the laser beam needs to be visible in the camera image. Considering LRFs with invisible laser beams, the authors present a method that extends the approach of Zhang and Pless for omnidirectional cameras.

A calibration of an omnidirectional camera to a 3D LRF without a calibration pattern was developed by Scaramuzza et al. [14]. Manual selection of correspondences in the laser data and camera image allow the computation of the rigid transformations between the selected points.

The calibration method introduced by Pandey et al. [15] uses a Velodyne HDL-64E with an omnidirectional camera. Therefore the authors extend the approach of Zhang and Pless [3] and use calibration patterns affixed to floors and walls.

3. HARDWARE

We use a Velodyne HDL-64E S2 LRF together with different cameras for our sensor platform. The Velodyne is a 3D LRF which rotates with up to 15 Hz around the upright axis. While rotating, 64 lasers permanently gather 3D distance measurements of the environment, up to 1.8 million points per second. One full rotation contains a point cloud dataset of about 120.000 points. In order to fuse the measurements with color and texture, we chose to use different types of cameras. We attached a Logitech HD Pro Webcam C910 to the front due to its wide angle and because we want to have a lot of pixels on the ground, e.g. for terrain classification tasks. To both sides of the platform we mounted each one Philips SPC1300NC webcam to detect dynamic objects such as pedestrians or vehicles approaching from the sides. The sensor platform is shown in Fig. 1 left and mounted on a car on the right.

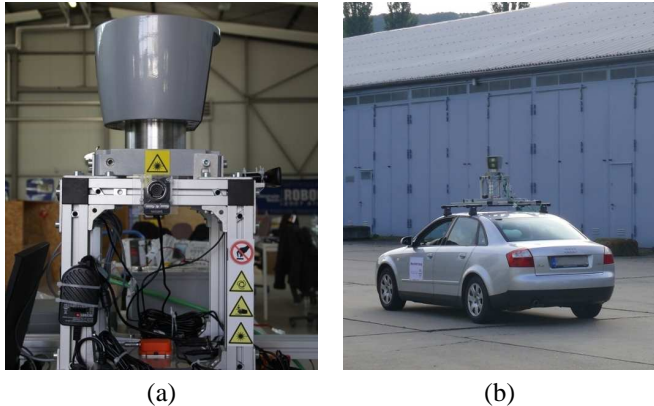


Fig. 1. Hardware setup. (a) shows our sensor platform with a Velodyne HDL-64E S2 mounted on top and different cameras adjusted to the sides. (b) displays the platform attached to a vehicle.

4. APPROACH

The approach of Unnikrishnan and Herbert [1] provides a fast and feasible calibration. It enables a simultaneous calibration of the intrinsic camera parameters as well as the rigid transformation of the camera in relation to the LRF. For the calibration a checkerboard is required and needs to be selected manually from the 3D data. Typically around 15 laser data / image pairs are required for a precise calibration, therefore the manual selection of the vertices for all three cameras takes a lot of time. As we wanted to reduce to necessary time spent on calibration to a minimum, we want a detection of our calibration object by all sensors as fast as possible. For this purpose, we performed several experiments and developed a calibration object matching our criteria.

4.1. CALIBRATION OBJECT

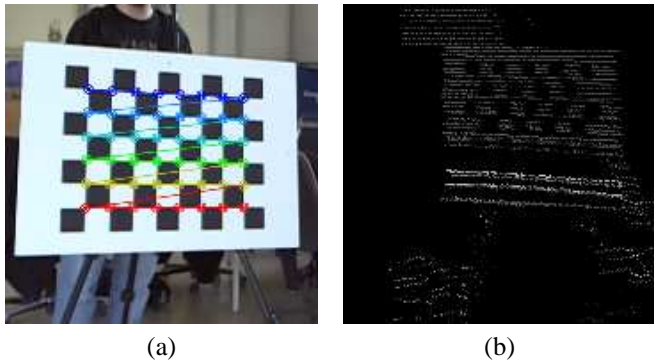


Fig. 2. Our calibration pattern. Actual sensor readings from the camera (a) and the laser range finder (b) point of view (after projection).

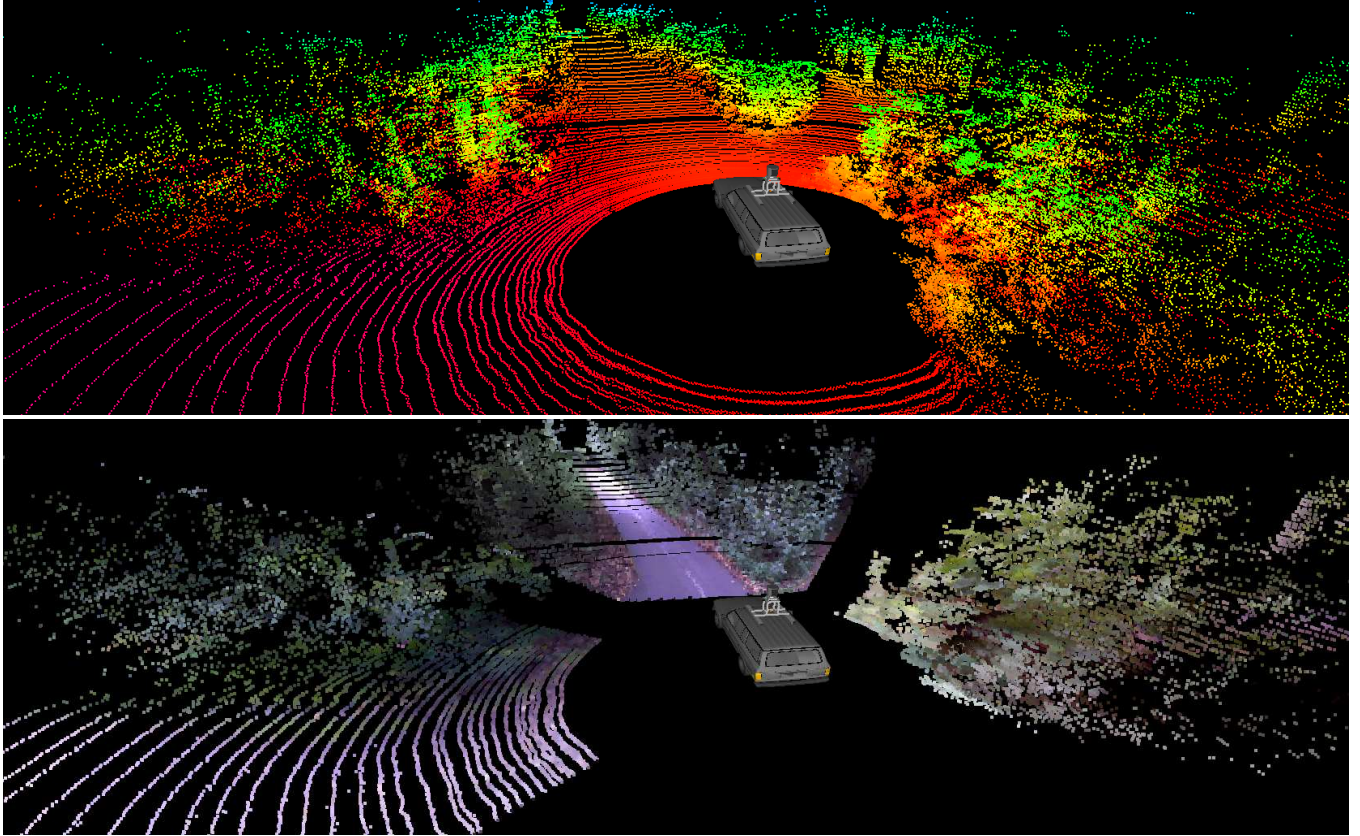


Fig. 3. Example scene of an unstructured environment. The 3D points are shown in the upper part where the color indicates the height. The image below presents the fusion of the three camera images with the 3D point cloud.

A fast or even automatic detection requires an object that is both visible in the LRF and camera data. On the one hand Andreasson et al. [4] point out that grey duct tape made their calibration frame detectable in the LRF data. On the other hand teams of the DARPA challenges report that black vehicles disappear completely in the laser data. Based on these reports we conducted various experiments with different material, surface structures and colors. Grey duct tape and matt black metallic surfaces almost completely absorb the intensity data of our LRF. Therefore we designed a calibration object made of a DIN A1 aluminium plate with a matt black checkerboard fixed on a camera tripod with flexible adjusting.

4.2. CALIBRATION

We make the premise that the 3D LRF is the center of the coordinate system. Hence, rotation \mathbf{R} and translation \mathbf{t} of a point \mathbf{P}_c from camera to laser coordinates is given by

$$\mathbf{P}_l = \mathbf{R}\mathbf{P}_c + \mathbf{t}. \quad (1)$$

Let $pair_{lc}$ be a set of a laser scan and the corresponding camera image. For each $pair_{lc}$ i we need to find orientation $(\theta_{c,i}, \theta_{l,i})$ and distance $(\delta_{c,i}, \delta_{l,i})$ of the planes

$\theta_{c,i}\mathbf{x} - \delta_{c,i} = 0$ and $\theta_{l,i}\mathbf{x} - \delta_{l,i} = 0$ to the camera respectively to the LRF. We extract $\theta_{c,i}$ and $\delta_{c,i}$ from the extrinsic calibration of the camera with the help of *OpenCV* (<http://opencv.willowgarage.com>). In order to retrieve $\theta_{l,i}$ and $\delta_{l,i}$, we have to locate the calibration object in the LRF data. The black patches create a checkerboard that is visible in the 3D intensity values (see Fig. 2 (b)) as we get no readings from our LRF. We used the information on which side of the LRF a camera is mounted to discard 50% of the points on the averted side. Additionally, we cull points that are too close to the LRF or which exceed the maximum range we chose for calibration. Afterwards we project all remaining points to a plane by discarding the depth value in the direction of the camera (front, left, right). This results in an “image” from the point of view of the camera on the laser data where the checkerboard is visible. Once the vertices of the calibration pattern are available, the projection can be reversed to retrieve the corresponding points in the 3D data.

Now, we have to find the transformation that minimizes the discrepancy between position and orientation of the calibration pattern in the camera and laser data. Therefore, we follow the approach of Unnikrishnan and Herbert [1] to opti-

mize

$$\underset{\mathbf{R}, \mathbf{t}}{\operatorname{argmin}} \sum_{i=1}^n \sum_{j=1}^{m(i)} \|\boldsymbol{\theta}_{c,i}^T(\mathbf{R}\mathbf{x}_{i,j} + \mathbf{t}) - \delta_{c,i}\|. \quad (2)$$

We have to have at least 15 *pair*_c for the calibration, which takes around 10 minutes for each camera. Since the calibration object can be folded, it is very portable and the sensor platform we use can be mounted easily on different vehicles. An example of the resulting fusion is presented in Fig. 3.

5. CONCLUSION

In this paper, we extended an existing approach to calibrate three cameras with a modern 3D LRF and adapted it to our domain. The calibration process could be improved by a new large matt black calibration object that can be detected in the camera images and in the 3D data with the help of projection and back projection. Resulting fused data were presented and the calibration process was described.

From the conducted experiments and calibration, some limitations of the approach revealed. Depending on the resolution of the cameras and the necessary minimal distance to the LRF, the checkerboard needs to be quite large. Therefore we recommend a minimum size of 20×20 cm for each patch, resulting in a calibration object of at least DIN A0. The matt black patches were detectable in the LRF data, but the angle of the checkerboard towards the LRF and illumination effects can disturb the detection outdoors.

6. REFERENCES

- [1] R. Unnikrishnan and M. Hebert, “Fast extrinsic calibration of a laser rangefinder to a camera,” Tech. Rep., Robotics Institute, Pittsburgh, USA, 2005.
- [2] D. Cobzaş, H. Zhang, and M. Jägersand, “A comparative analysis of geometric and image-based volumetric and intensity data registration algorithms,” in *Proceedings of the IEEE International Conference on Intelligent Robots and Systems*, Washington, USA, 2002, pp. 2506–2511.
- [3] Q. Zhang and R. Pless, “Extrinsic calibration of a camera and laser range finder,” in *Proceedings of the IEEE International Conference on Intelligent Robots and Systems*, Sendai, Japan, 2004, pp. 2301–2306.
- [4] H. Andreasson, R. Triebel, and A. Lilienthal, *Non-iterative Vision-based Interpolation of 3D Laser Scans*, pp. 83–90, Springer, Germany, 2007.
- [5] J. Leonard, D. Barrett, J. How, S. Teller, M. Antone, S. Campbell, A. Epstein, G. Fiore, L. Fletcher, E. Frazzoli, A. Huang, T. Jones, O. Koch, Y. Kuwata, K. Mahelona, D. Moore, K. Moyer, E. Olson, S. Peters, C. Sanders, J. Teo, and M. Walter, “Team MIT urban challenge technical report,” Tech. Rep. MIT-CSAIL-TR-2007-058, Massachusetts Institute of Technology, Cambridge, USA, 2007.
- [6] V. Caglioti, A. Giusti, and D. Migliore, “Mutual calibration of a camera and a laser rangefinder,” in *VIS-APP (Workshop on Robot Perception)*, Funchal, Portugal, 2008, pp. 33–42.
- [7] C. Colombo, D. Comanducci, and A. del Bimbo, “Camera calibration with two arbitrary coaxial circles,” in *Proceedings of the 9th European Conference on Computer Vision*, Graz, Austria, 2006, pp. 265–276.
- [8] P. Nůñez, P. Drews Jr, R. Rocha, and J. Dias, “Data fusion calibration for a 3d laser range finder and a camera using inertial data,” in *Proceedings of the 4th European Conference on Mobile Robots (ECMR)*, Mlini/Dubrovnik, Croatia, 2009, pp. 31–36.
- [9] R. Horaud and F. Dornaika, “Hand-eye calibration,” *International Journal of Robotics Research*, vol. 14, no. 3, pp. 195–210, 1995.
- [10] G. Li, Y. Liu, L. Dong, X. Cai, and D. Zhou, “An algorithm for extrinsic parameters calibration of a camera and a laser range finder using line features,” in *Proceedings of the IEEE/RSJ International Conference on Intelligent Robots and Systems*, 2007, pp. 3854–3859.
- [11] H. Aliakbarpour, P. Nůñez, J. Prado, K. Khoshhal, and J. Dias, “An efficient algorithm for extrinsic calibration between a 3d laser range finder and a stereo camera for surveillance,” in *Proceedings of the 14th International Conference on Advanced Robotics*, Munich, Germany, 2009, pp. 3854–3859.
- [12] T. Svoboda, D. Martinec, and T. Pajdla, “A convenient multi-camera self-calibration for virtual environments,” *Presence: Teleoperators and Virtual Environments*, vol. 14, no. 4, pp. 407–422, 2005.
- [13] C. Mei and P. Rives, “Calibration between a central catadioptric camera and a laser range finder for robotic applications,” in *Proceedings of the IEEE International Conference on Robotics and Automation*, Orlando, USA, 2006, pp. 532–537.
- [14] D. Scaramuzza, A. Harati, and R. Siegwart, “Extrinsic self calibration of a camera and a 3d laser range finder from natural scenes,” in *Proceedings of the IEEE/RSJ International Conference on Intelligent Robots and Systems*, 2007, pp. 4164–4169.
- [15] G. Pandey, J. McBride, S. Savarese, and R. Eustice, “Extrinsic calibration of a 3d laser scanner and an omnidirectional camera,” in *7th IFAC Symposium on Intelligent Autonomous Vehicles*, Lecce, Italy, 2010.